OPEN

Citation: Cell Death and Disease (2014) 5, e1113; doi:10.1038/cddis.2014.86

www.nature.com/cddis

BAX inhibitor-1-associated V-ATPase glycosylation enhances collagen degradation in pulmonary fibrosis

M-R Lee[1,5], G-H Lee[1,5], H-Y Lee[1], D-S Kim[1], MJ Chung[2], YC Lee[3], H-R Kim*[,4] and H-J Chae*[,1]

Endoplasmic reticulum (ER) stress is considered one of the pathological mechanisms of idiopathic pulmonary fibrosis (IPF). Therefore, we examined whether an ER stress regulator, Bax inhibitor-1 (BI-1), regulates collagen accumulation, which is both a marker of fibrosis and a pathological mechanism of fibrosis. The presence of BI-1 inhibited the transforming growth factor-β1-induced epithelial–mesenchymal transition of epithelial pulmonary cells and bleomycin-induced pulmonary fibrosis in a mouse model by enhancing collagen degradation, most likely by enhanced activation of the lysosomal V-ATPase through glycosylation. We also found a correlation between post-translational glycosylation of the V-ATPase and its associated chaperone, calnexin, in BI-1-overexpressing cells. BI-1-induced degradation of collagen through lysosomal V-ATPase glycosylation and the involvement of calnexin were confirmed in a bleomycin-induced fibrosis mouse model. These results highlight the regulatory role of BI-1 in IPF and reveal for the first time the role of lysosomal V-ATPase glycosylation in IPF.
Cell Death and Disease (2014) **5,** e1113; doi:10.1038/cddis.2014.86; published online 13 March 2014
Subject Category: Immunity

Idiopathic pulmonary fibrosis (IPF) is a chronic, progressive, and fatal form of interstitial lung disease.[1] Pulmonary fibrosis results from chronic damage to the lungs in conjunction with the accumulation of extracellular matrix (ECM) proteins.[2,3] After an acute lung injury, lung epithelial cells regenerate and replace necrotic or apoptotic cells. If lung injury persists, epithelial cells undergo a phenotypic transformation to become myofibroblast-like and secrete an ECM composed of various proteins, such as collagen type I.[4] Collagen is a secretory protein that is transferred to the Golgi and secreted into the ECM; collagen accumulation in the ECM is considered a direct mechanism of IPF.[5] Despite numerous studies of collagen accumulation and its role in IPF, the molecular mechanisms remain unknown. However, a few studies have indicated that endoplasmic reticulum (ER) stress, caused by apoptosis of alveolar epithelial cells, is involved in the pathogenesis of pulmonary fibrosis.[6–8] In addition, evidence of ER stress has been found in the lungs of patients with familial and sporadic IPF.[9] Recent studies also examined how ER stress is induced in IPF.[10,11] Under the ER stress, an overload of proteins to be folded or the accumulation of misfolded proteins adversely affects processes required for appropriate or efficient folding, such as glycosylation.

ER stress response is regulated by Bax inhibitor-1 (BI-1), an anti-apoptotic protein capable of inhibiting Bax activation and translocation to the mitochondria.[12] Physiologically, BI-1 is linked to the dynamic Ca^{2+} environment of the ER.[13,14] Dynamic Ca^{2+} status is linked to chaperones, such as calnexin and calreticulin.[15] Calnexin has an important role in glycoprotein folding as a lectin-like chaperone;[16] together with calreticulin, it performs quality control by retaining incompletely folded or misfolded proteins in the ER.[17,18] Our hypothesis was that the expression levels of BI-1-associated ER chaperones change according to the dynamic Ca^{2+} status in BI-1-overexpressing cells (BI-1 cells), leading to an increase in the folding capacity of the ER. To test our hypothesis, we examined BI-1-associated ER stress regulation and the intra-ER protein folding process in both *in vitro* and *in vivo* fibrosis models.

Results

BI-1 regulates the transforming growth factor (TGF)-β1-induced epithelial–mesenchymal transition (EMT) in epithelial pulmonary cells. A recent study proposed that ER stress is involved in IPF and that chemical regulation of ER stress may be a potential therapy for IPF.[19] In this study, we examined the effect of the endogenous ER stress regulator, BI-1, on the TGF-β1-induced EMT, in an *in vitro* model of IPF. In response to TGF-β1 treatment,

[1]Department of Pharmacology and Institute of Cardiovascular Research, Medical School, Chonbuk National University, Jeonju, Chonbuk, Republic of Korea; [2]Department of Pathology, Chonbuk National University Medical School, Jeonju, Chonbuk, Republic of Korea; [3]Department of Internal Medicine, Chonbuk National University, Medical School, Jeonju, Chonbuk, Republic of Korea and [4]Department of Dental Pharmacology, School of Dentistry, Wonkwang University, Iksan, Chonbuk, Republic of Korea
*Corresponding author: H-R Kim, Department of Dental Pharmacology, School of Dentistry, Wonkwang University, Iksan, Chonbuk 570-749, Republic of Korea. Tel: +82 63 850 6640; Fax: +82 63 854 8725; E-mail: hrkimdp@wonkwang.ac.kr
or H-J Chae, Department of Pharmacology, School of Medicine, Chonbuk National University, Jeonju, Chonbuk 560-182, Republic of Korea. Tel: +82 63 270 3092; Fax: +82 63 275 2855; E-mail: hjchae@chonbuk.ac.kr
[5]These authors contributed equally to this work.
Keywords: idiopathic pulmonary fibrosis; BI-1; epithelial—mesenchymal transition; ER stress; lysosome; V-ATPase glycosylation
Abbreviations: ER, endoplasmic reticulum; IPF, idiopathic pulmonary fibrosis; BI-1, Bax inhibitor-1; TGF, transforming growth factor; ECM, extracellular matrix; α-SMA, α-smooth muscle actin; EMT, epithelial–mesenchymal transition; PNGase-F, peptide *N*-glycosidase-F; UGGT, UDP-glucose:glycoprotein glucosyltransferase
Received 18.11.13; revised 01.2.14; accepted 06.2.14; Edited by M Agostini

neomycin-resistant vector-transfected cells (Neo cells) showed a decrease in cell-to-cell contacts and became more elongated, whereas BI-1 cells had a pebble-like shape and cell–cell adhesion, structural changes that are associated with the EMT (Figure 1a). Viability of Neo cells and BI-1 cells was similar, regardless of the presence or absence of TGF-β1 (Supplementary Figure S1). Fluorescence microscopy (Figure 1b) and immunoblotting analysis (Figure 1c) demonstrated that expression levels of N-cadherin, β-catenin, α-smooth muscle actin (α-SMA), and vimentin increased less after TGF-β1 treatment in BI-1 cells than in Neo cells. E-cadherin was more significantly increased in TGF-β1-treated BI-1 cells than in Neo cells, suggesting that expression of BI-1 regulates the TGF-β1-induced EMT.

BI-1 regulates TGF-β1-induced collagen expression and secretion through lysosomal activation. Collagen accumulation is a direct pathological mechanism of fibrosis.[20] In this study, we stained Neo and BI-1 cells for intracellular collagen with antibodies against collagen 1A1.

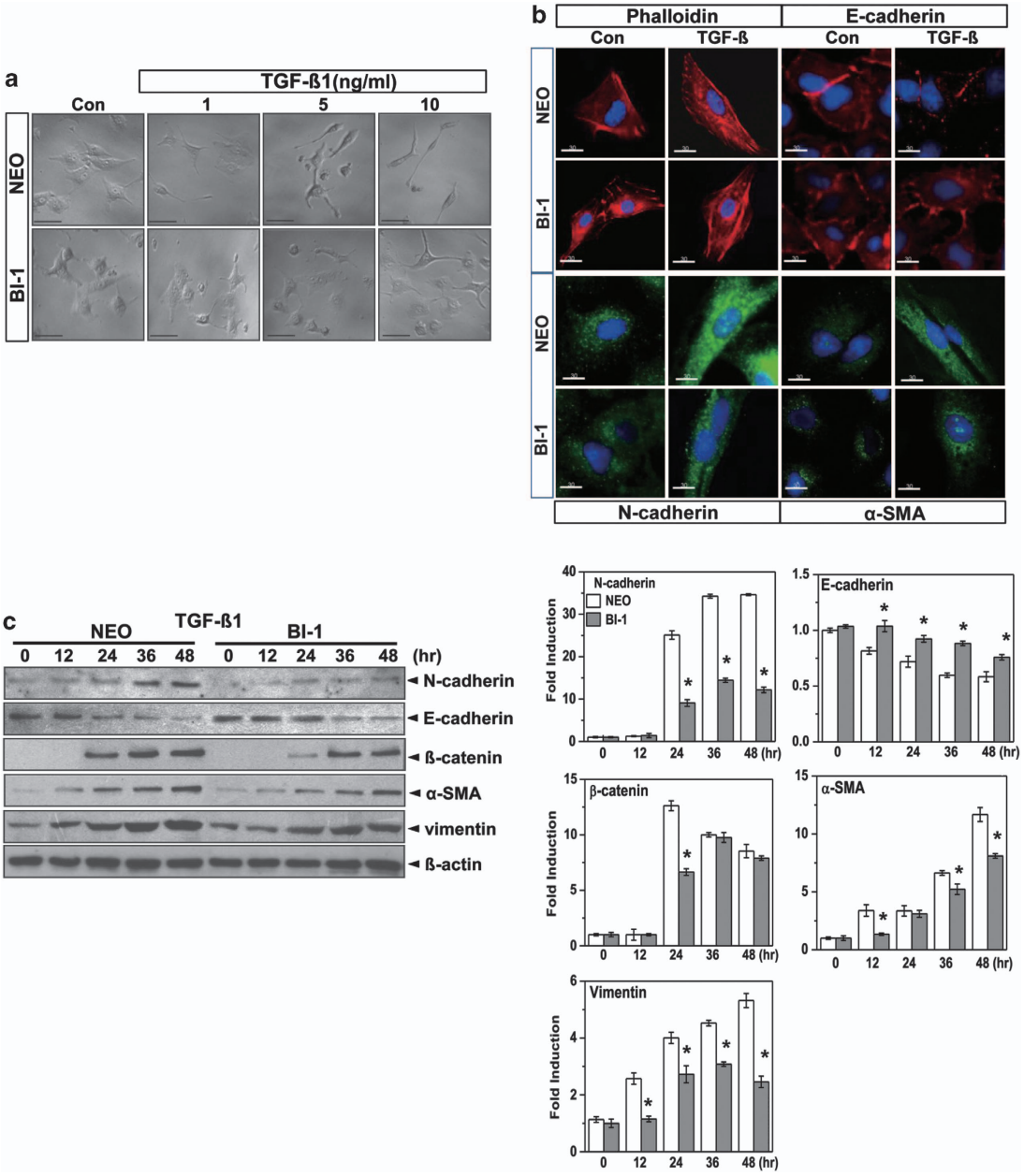

Figure 1 BI-1 regulates the TGF-β1-induced EMT. (**a**) Neo and BI-1 cells were cultured in serum-free medium with or without 1, 5, and 10 ng/ml TGF-β1 for 48 h. Cellular morphology was then photographed under a light microscope. (**b**) Neo and BI-1 cells were cultured in serum-free medium with or without 5 ng/ml TGF-β1. Phalloidin (red), E-cadherin (red), N-cadherin (green), or α-SMA (green), together with nuclei (blue), were stained and photographed under a fluorescent microscope. (**c**) Cells were cultured in serum-free medium with or without 5 ng/ml TGF-β1 for 0, 12, 24, 36, or 48 h. Cell lysates were then immunoblotted using anti-E-cadherin, N-cadherin, β-catenin, α-SMA, or vimentin antibodies. β-Actin from the same loading was used as a control. *$P<0.05$ *versus* Neo cells at each time point

Under TGF-β1, BI-1 cells had accumulated less intracellular collagen than Neo cells (Figure 2a). Soluble collagen in the Neo cells and their medium increased in a time-dependent fashion but increased significantly less in BI-1 cells (Figure 2b). There was less cellular accumulation of hyroxyproline, showing more secretion of hydroxyproline in the BI-1 cells than in Neo cells (Figure 2c). And then, we analyzed collagen transcript levels using real-time PCR. We found a significant increase in collagen mRNA levels following TGF-β1 treatment in both cell types, with no differences in transcript levels between Neo and BI-1 cells (Figure 2d). Because there were no differences in the rate of mRNA transcription or protein synthesis (determined by methionine-labeled protein synthesis analysis and shown in Figure 2e) between Neo and BI-1 cells, we next examined the post-translational protein degradation pathway. The lysosomal enzyme inhibitors bafilomycin and pepstatin A, but not the proteasome inhibitors lactacystin and MG132, reversed the BI-1-induced regulation of collagen in cells and their media (Figure 2f). Similarly, lysosomal inhibition reversed the comparatively low levels of hydroxyproline expression and secretion in BI-1 cells (Figure 2g). Next, we directly compared lysosomal activity-associated collagen degradation between Neo and BI-1 cells. Purified collagen was incubated with lysosomal fractions from both cell types. As expected, degradation of collagen α1 and α2, main components of type I collagen,[21] occurred to a greater extent when the lysosomal fraction from TGF-β1-treated BI-1 cells was added than when that from treated Neo cells was added (Figure 2h). These data suggest that the BI-1-associated regulation of the EMT involves the lysosomal pathway, not the proteasomal pathway.

BI-1 cells showed high lysosomal activity that was maintained following TGF-β1 treatment, leading to the regulated ER stress response. Next, we measured BI-1-associated lysosomal activity. Basally, lysosomal fluorescence or integrity was higher in BI-1 cells than in Neo cells (Supplementary Figure S2). In the presence of TGF-β1, lysosomal integrity and volume increased transiently in Neo cells, especially within the first 12-h period. In BI-1 cells, fluorescence intensity and volume were stably high with or without TGF-β1 treatment (Figure 3a). To determine the role of lysosomes, we analyzed the activity of the lysosomal enzyme, cathepsin B. In Neo cells, the activity of cathepsin B was slightly increased by treatment with TGF-β1 and returned to a level lower than that in the control (Figure 3b). In BI-1 cells, the activity of cathepsin B was stably high in the presence or absence of TGF-β1. Analysis of enzyme activity in lysosomal extracts revealed that lysosomal V-ATPase activity was basally higher in BI-1 cells than in Neo cells, with or without TGF-β1 (Figure 3c). A time–kinetic analysis of V-ATPase activity in response to TGF-β1 treatment indicated that the lysosomal V-ATPase was highly activated and relatively more stable in BI-1 cells than in Neo cells (Figure 3d).

We also assessed the activity of three glycosylation-associated lysosomal enzymes in Neo and BI-1 cells: β-galactosidase, α-mannosidase, and β-glucuronidase. Basal expression levels of β-galactosidase and β-glucuronidase were higher in BI-1 cells than in Neo cells (Figure 3e). All three lysosomal glycosylation enzymes were more highly activated in TGF-β1-treated BI-1 cells than in treated Neo cells. Proteasome activity and expression were also comparable between Neo and BI-1 cells. Chymotrypsin enzyme activity and 20S proteasome expression were not significantly different between Neo and BI-1 cells, regardless of TGF-β1 treatment (Supplementary Figures S3a and b).

To understand whether lysosomal enzymes, especially V-ATPase, are involved in regulation of the ER stress response, we pre-exposed TGF-β1-treated BI-1 cells to the V-ATPase inhibitor bafilomycin (10 nM, a non-toxic concentration around the half-maximal inhibitory concentration) or V-ATPase small interfering RNA (siRNA).[22] As shown in Figure 4a, there was less of an ER stress response (GRP78, CHOP, IRE-1α, spliced XBP-1, PERK, p-eIF2α, p-JNK, and ATF6α) after TGF-β1 treatment in BI-1 cells than in Neo cells. In the presence of bafilomycin A, however, the reduced ER stress response was significantly reversed, especially in BI-1 cells (Figure 4b). Consistently, in V-ATPase siRNA-transfected cells, the reduced ER stress response was reversed, especially in BI-1 cells (Figure 4c), suggesting that enhanced activity of lysosomal enzymes such as V-ATPase contributes to BI-1-induced ER stress regulation.

BI-1 stimulation of V-ATPase glycosylation involves calnexin and calreticulin expression. When V-ATPase, an *N*-acetylglycosylated protein,[23] is appropriately glycosylated, it is localized to the lysosome, where it performs its endogenous functions such as intra-organelle acidification, which promotes protein degradation. Cells were first immunostained with V01 antibody against the glycosylated subunit of V-ATPase. A glycosylation pattern was clearly observed in BI-1 cells as compared with Neo cells, with or without TGF-β1 treatment (Supplementary Figure S4). Expression of glycosylated V-ATPase was decreased in Neo cells treated with TGF-β1 compared with untreated cells (Figure 5a). However, glycosylated V-ATPase expression was higher and more stable in BI-1 cells than in Neo cells. Glycosylated form of V-ATPase in the lysosomal fraction was higher in non-treated BI-1 cells than in Neo cells, and glycosylation was stably maintained in TGF-β1-treated BI-1 cells as compared with treated Neo cells (Figure 5b). Glycosylated V-ATPase was expressed at a lower level in the ER fraction of TGF-β1-treated BI-1 cells than in the ER fraction of Neo cells, suggesting more efficient translocation of glycosylated V-ATPase into the lysosome in TGF-β1-treated BI-1 cells. Expression of glycosylated V-ATPase and LAMP-1 overlapped more often in BI-1 cells, especially in the presence of TGF-β1, than in Neo cells (Figure 5c). Overlapping expression of glycosylated V-ATPase with calnexin, an ER marker protein, was consistently lower in TGF-β1-treated BI-1 cells than in treated Neo cells.

To obtain information about the glycan composition of V-ATPase, we used O-glynase, endoglycosidase-H, and peptide *N*-glycosidase-F (PNGase-F). Glycosylation of V-ATPase was abrogated in the presence of PNGase-F, but not in the presence of O-glynase or endoglycosidase-H, suggesting that PNGase-F-sensitive complex type *N*-glycosylation is involved in post-translational modification of the

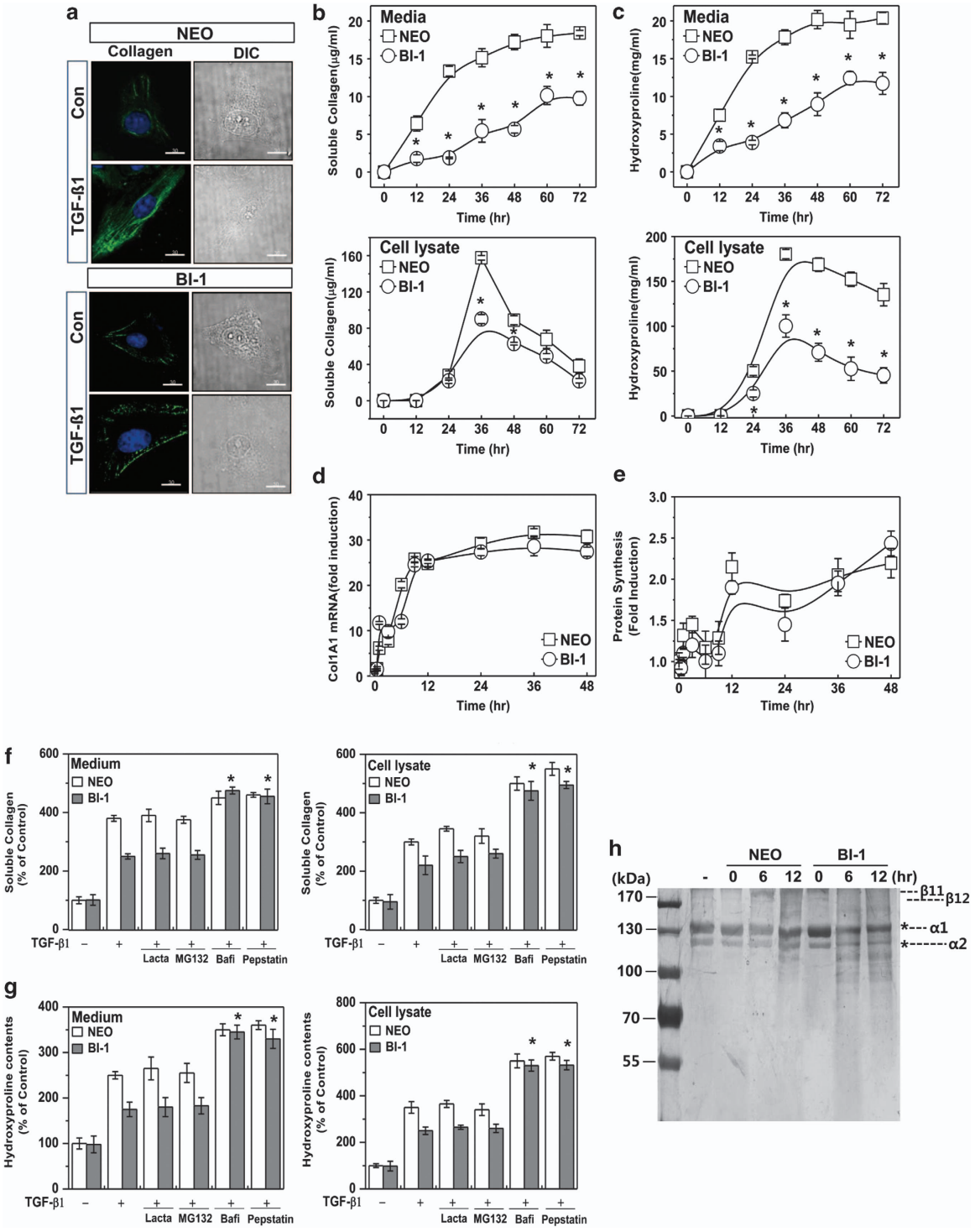

Figure 2 BI-1 attenuates TGF-β1-induced collagen accumulation through lysosomal activation. (**a**) Neo and BI-1 cells were cultured in serum-free medium with or without 5 ng/ml TGF-β1 for 48 h. Intracellular collagen was stained with anti-collagen 1A1 antibody and photographed under a fluorescent microscope. Neo and BI-1 cells were then cultured in serum-free medium with or without 5 ng/ml TGF-β1 for 0, 12, 24, 36, 48, 60, or 72 h. (**b**) Soluble collagen and (**c**) hydroxyproline assays of the medium and cell lysate were performed as described in the Materials and Methods. (**d**) Real-time PCR analysis and (**e**) methionine-labeled protein synthesis analysis were performed. Next, Neo and BI-1 cells were incubated with or without 5 ng/ml TGF-β1 for 36 h in the presence or absence of proteasome inhibitors (2 μM MG132 or 5 μM lactacystin) or lysosome inhibitors (10 μg/ml pepstatin or 100 nM bafilomycin A). (**f**) Soluble collagen and (**g**) hydroxyproline assays of the medium and cell lysate were performed as described in the Materials and Methods. (**h**) Collagen purified from rat tails was incubated with lysosome fractions from TGF-β1-treated or non-treated Neo or BI-1 cells for 30 min. Silver staining was performed as described in the Materials and Methods. *$P<0.05$ *versus* TGF-β1-treated BI-1 cells without inhibitors. Bafi, bafilomycin; Lacta, lactacystin

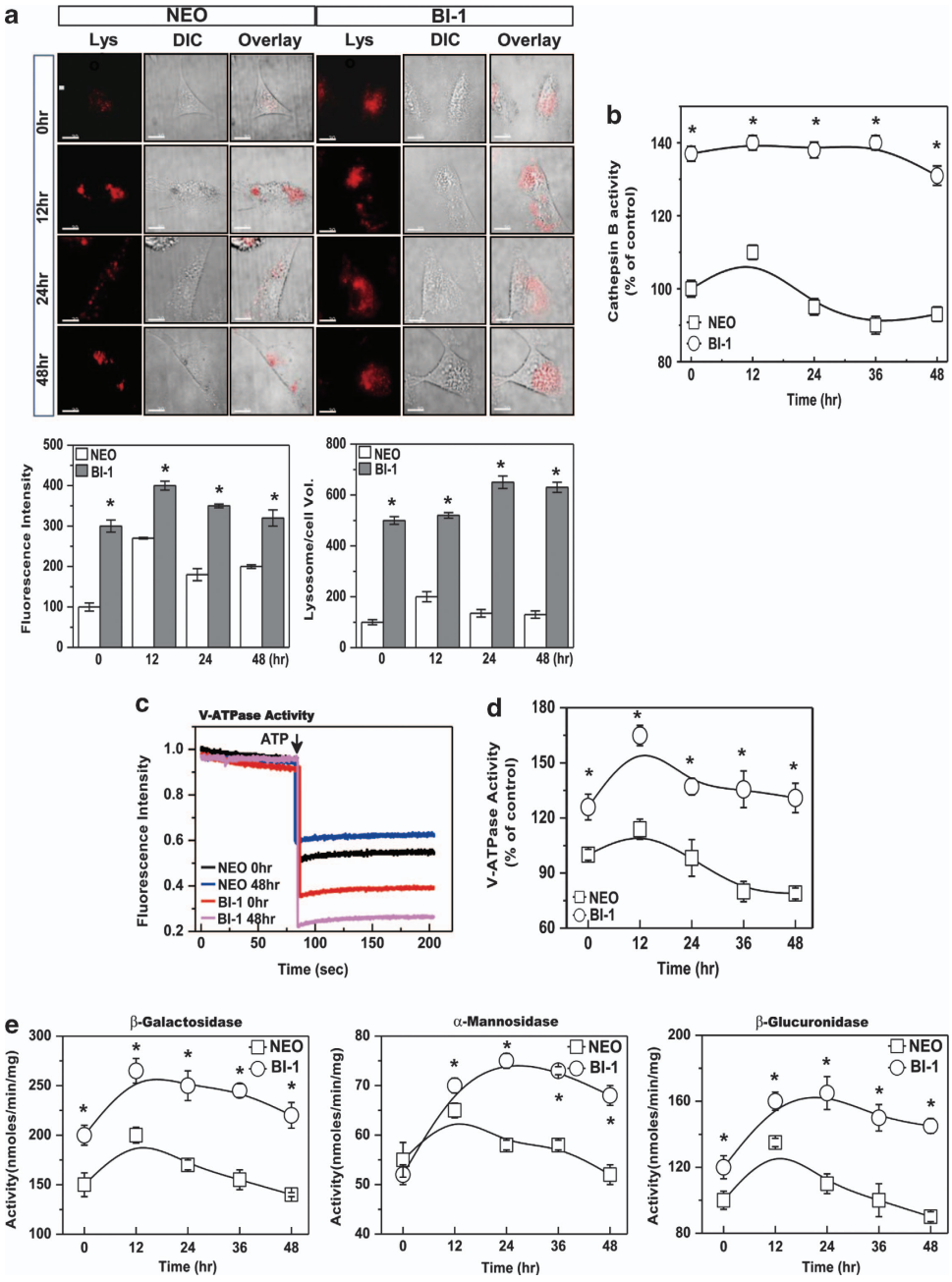

Figure 3 BI-1 is associated with high lysosomal activity. (**a**) Neo and BI-1 cells were cultured in serum-free medium with or without 5 ng/ml TGF-β1 for 0, 12, 24, or 48 h. Then, cells were exposed to 5 μM LysoTracker and photographed. Scale bar, 30 μm. Fluorescence intensity and volume were quantified (bottom). *$P<0.05$, significantly different from Neo cells at each point. (**b**) After isolation of lysozymes, cathepsin B was analyzed. For lysosomal V-ATPase activity, 6 μM acridine orange solution was added to lysosomal membranes from Neo and BI-1 cells that were untreated or treated with TGF-β1 for 48 h. (**c**) Intra-vesicular H^+ uptake was initiated by the addition of Mg-ATP, and fluorescence was measured as described in the Materials and Methods. (**d**) V-ATPase activity was quantified in TGF-β1-treated and non-treated Neo and BI-1 cells for the indicated periods. (**e**) β-Galactosidase, α-mannosidase, and β-glucuronidase activity in the lysosomal extracts was measured using a spectrofluorospectrometer. Lys, LysoTracker

V-ATPase (Figure 6a). We also measured V-ATPase activity in the presence of PNGase-F, a positive regulator of BI-1-induced V-ATPase glycosylation. Enhanced V-ATPase activity of TGF-β1-treated BI-1 cells was significantly inhibited in the presence of PNGase-F, especially compared with the treated Neo cells (Figure 6b). To confirm the V-ATPase glycosylation-induced increase in collagen degradation, purified collagen was incubated with lysosome fractions from Neo or BI-1 cells in the presence or absence of PNGase-F. Collagen was significantly degraded by incubation with the lysosomal fraction from TGF-β1-treated BI-1 cells, as revealed by smear patterns in the gels (Figure 6c). However, treatment of these cells with PNGase-F significantly reversed the degradation pattern. To determine the glycosylation characteristics of BI-1 cells, we analyzed the activities of specific glycosylation enzymes. Activities of the *N*-acetylglycosylation-associated

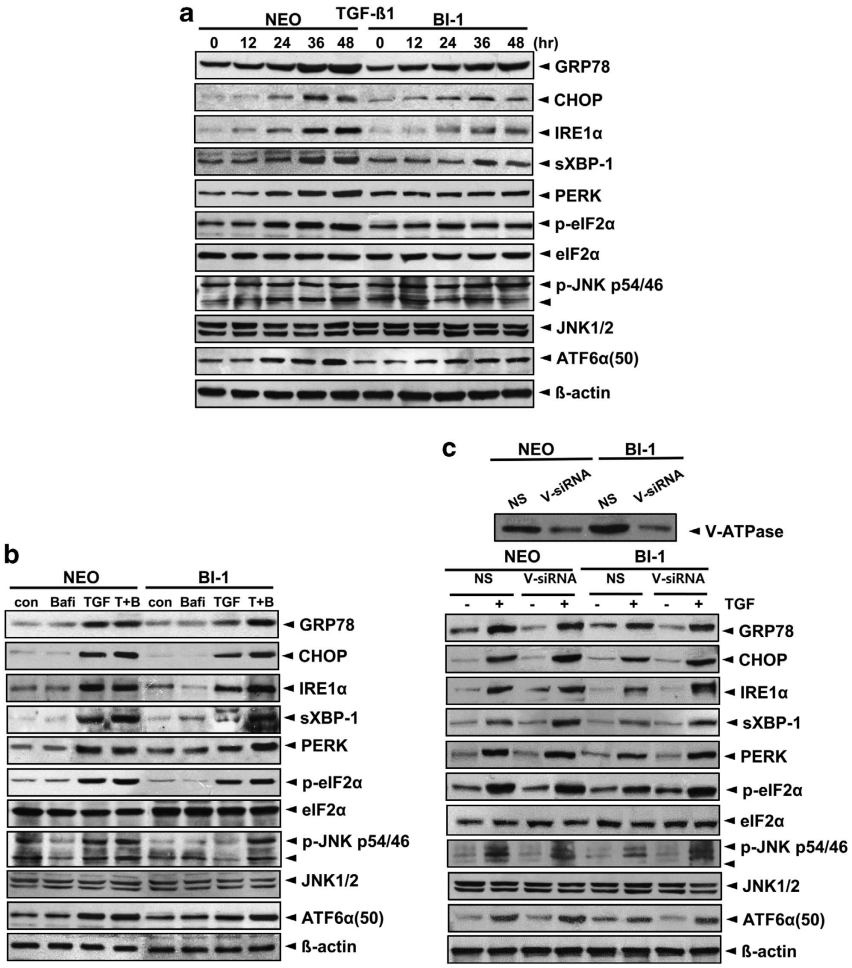

Figure 4 BI-1-associated lysosomal activity leads to ER stress regulation. (**a**) Neo and BI-1 cells were cultured in serum-free medium with 10 ng/ml TGF-β1 for 0, 12, 24, 36, or 48 h. (**b**) Neo and BI-1 cells were cultured in serum-free medium with 10 ng/ml TGF-β1 in the presence or absence of 10 nM bafilomycin for 48 h. Neo and BI-1 cells were transfected with non-specific or V-ATPase specific siRNA and immunoblotting was performed with anti-V-ATPase antibody. (**c**) Separately, siRNA-transfected Neo and BI-1 cells were cultured in serum-free medium with 10 ng/ml TGF-β1 for 48 h. Immunoblotting was performed with anti-GRP78, CHOP, IRE-1α, sXBP-1, PERK, p-eIF2α, eIF2α, p-JNK, JNK1, ATF6α (50KD), and β-actin antibodies. NS, non-specific siRNA; V-siRNA, V-ATPase siRNA

enzymes, α-glucosidase and ER-resident mannosidase, were significantly higher in the ER fractions of BI-1 cells than those of Neo cells (Figure 6d). UDP-glucose:glycoprotein glucosyltransferase (UGGT) functions as a central gatekeeper for ER quality control of glycoproteins, because it recognizes partially folded proteins as substrates and reglucosylates deglucosylated N-glycans, facilitating another round of interaction with calreticulin and calnexin. In the presence of TGF-β1, the activity of UGGT decreased during the first 12 h and then recovered sharply in Neo cells, whereas its activity was consistently lower in BI-1 cells than in treated Neo cells.

Chaperone proteins calreticulin and calnexin are essential for the activation of glucosidase, a rate-limiting step in N-glycosylation.[24] Therefore, we examined the expression of calreticulin and calnexin with and without TGF-β1. Treatment with TGF-β1 induced calnexin expression in BI-1 cells more strongly than it did in Neo cells (Figure 6e). Immunoprecipitation assays (Figure 6f) showed that V-ATPase interacted specifically with calnexin in a manner that was similar in both untreated Neo cells and BI-1 cells. TGF-β1 treatment of BI-1 cells, however, significantly decreased the V-ATPase–calnexin interaction at 48 h, suggesting that V-ATPase may have been translocated to the lysosome or, at the least, may have exited from the ER by that time point.

BI-1 regulates bleomycin-induced pulmonary fibrosis. To understand the function of BI-1 *in vivo*, we investigated bleomycin-induced fibrosis in BI-1 knockout mice. BI-1$^{-/-}$ mice exhibited high sensitivity and low survival in response to bleomycin treatment (Supplementary Figure S5a). Body weight was more severely reduced in mice in the BI-1$^{-/-}$ group than mice in the BI-1$^{+/+}$ group (Supplementary Figure S5b). BI-1$^{+/+}$ and BI-1$^{-/-}$ mice were treated with intratracheal injections of bleomycin for 2 and 4 weeks, respectively. In axial slices of micro-CT scans of fibrotic lungs from bleomycin-instilled BI-1$^{+/+}$ and BI-1$^{-/-}$ mice, the lung densities of the BI-1$^{-/-}$ mice treated with bleomycin for 2 or 4 weeks were greater than those in the corresponding BI-1$^{+/+}$ mice (Figure 7a). Hematoxylin and eosin staining revealed a decrease in the width of the interstitial areas in BI-1$^{-/-}$ mice treated with bleomycin for 4 weeks compared

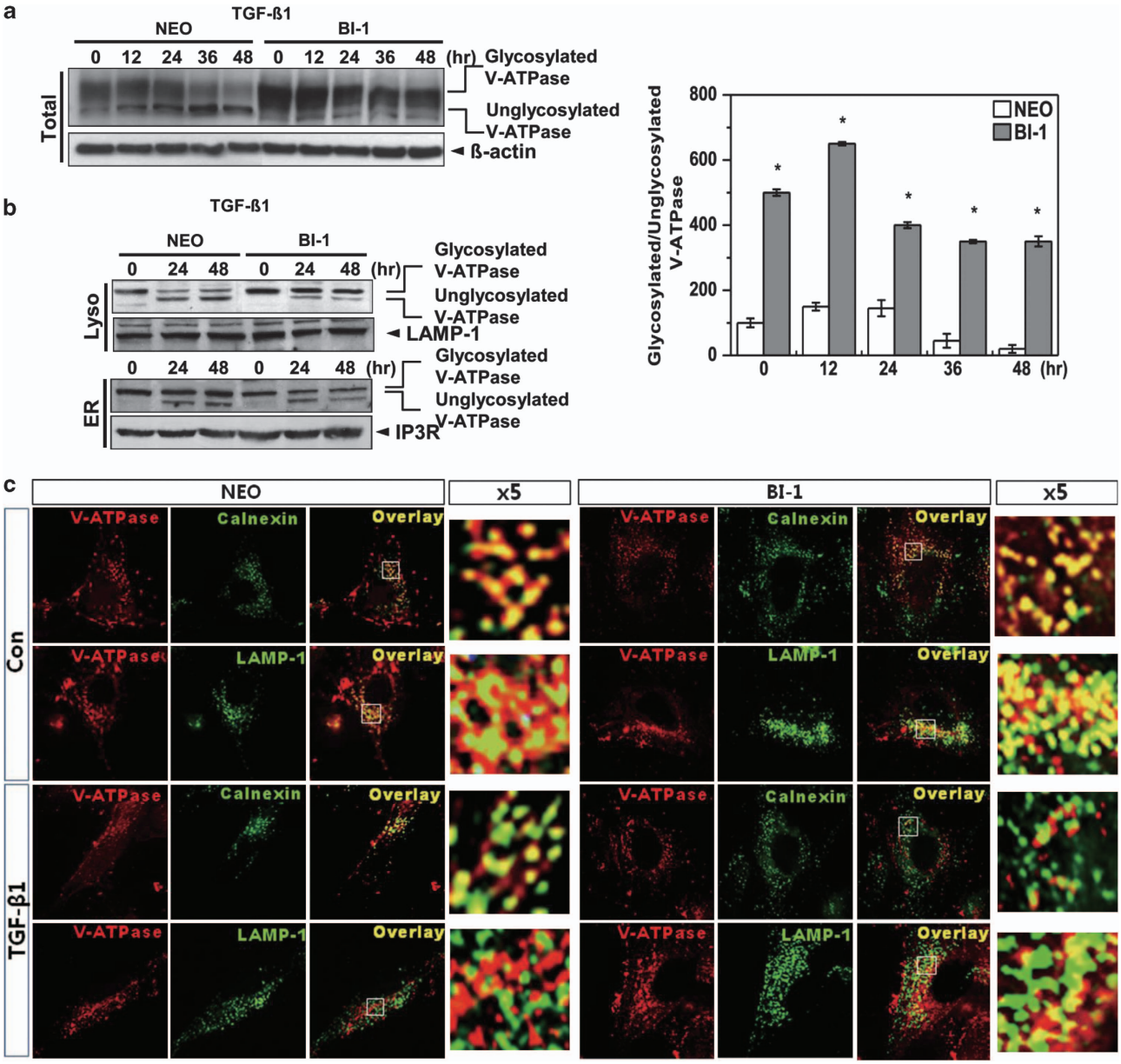

Figure 5 Lysosomal V-ATPase is highly expressed in BI-1 cells. (**a**) Neo and BI-1 cells were cultured in serum-free medium with or without 5 ng/ml TGF-β1 for 0, 12, 24, 36, or 48 h. Immunoblotting was performed with antibodies against the V-ATPase V0a1 subunit or β-actin. Ratio of glycosylated to unglycosylated V-ATPase was quantified as shown in the right panel. *$P<0.05$, significantly different from Neo cells during each period. (**b**) Neo and BI-1 cells were cultured in serum-free medium with or without 5 ng/ml TGF-β1 for 0, 24, or 48 h. After the lysosome and ER fractions were isolated, immunoblotting was performed using anti-V-ATPase V0a1 subunits, LAMP-1, or IP3R antibodies. (**c**) Neo and BI-1 cells were cultured in serum-free medium with or without 5 ng/ml TGF-β1 for 48 h. Immunostaining with anti-V-ATPase, calnexin, or LAMP-1 antibodies was performed, and the images were captured under a fluorescent microscope

with that of BI-1$^{+/+}$ mice treated with bleomycin for the same length of time (Figure 7b). Alveolar septum widths were also smaller in bleomycin-treated BI-1$^{-/-}$ mice than in bleomycin-treated BI-1$^{+/+}$ mice. To determine whether fibrosis was occurring, we stained for collagen with Masson's trichrome stain. Bleomycin-treated BI-1$^{-/-}$ mice had a much clearer collagen staining pattern than bleomycin-treated BI-1$^{+/+}$ mice (Figure 7c), suggesting an increase in fibrosis in the lungs of BI-1$^{-/-}$ mice. Lung collagen levels and hydroxyproline content were also significantly higher in the BI-1$^{-/-}$ group than in the BI-1$^{+/+}$ group (Figures 7d and e). N-cadherin, β-catenin, α-SMA, and vimentin were highly expressed in the lungs of bleomycin-treated BI-1$^{-/-}$ mice, but E-cadherin was expressed at low levels in BI-1$^{-/-}$ mice, reflecting pathological EMT changes (Figure 7f). Immunohistochemical analysis showed that α-SMA and vimentin were consistently more highly expressed in the lungs of BI-1$^{-/-}$ mice than in the lungs of the BI-1$^{+/+}$ mice (Figure 7g).

To assess the biological role of the ER stress response in pulmonary fibrosis, we examined the expression of GRP78 in bleomycin-treated mouse lung tissues. GRP78 was more

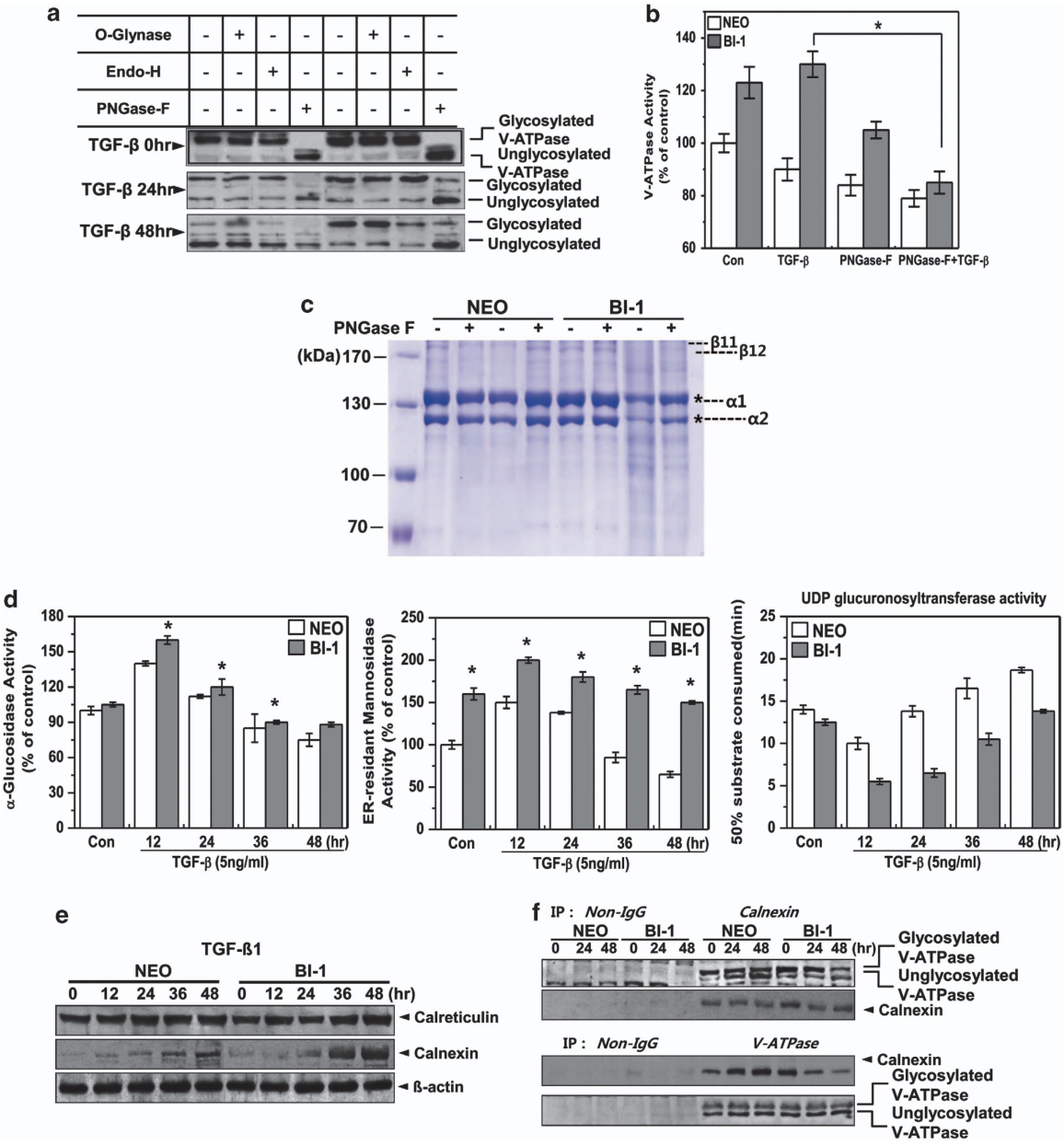

Figure 6 BI-1 enhances N-glycosylation activity in the ER during TGF-β1 treatment. (**a**) Neo and BI-1 cells were cultured with 5 ng/ml TGF-β1 for 0, 24, or 48 h. O-glynase, Endo-H, or PNGase-F was added to the extracts followed by 30-min incubation. Immunoblotting was then performed with anti-V-ATPase antibody. (**b**) V-ATPase activity in the lysosome fractions isolated from 5 ng/ml TGF-β1-treated Neo or BI-1 cells in the presence or absence of PNGase-F was measured and quantified. *$P<0.05$, significantly different from TGF-β1-treated BI-1 cells. (**c**) Purified collagens from rat tails were incubated with lysosome fractions from TGF-β1-treated or non-treated Neo or BI-1 cells in the presence or absence of PNGase-F. Coomassie staining was performed as described in the Materials and Methods. *; α1 or α2 collagen. (**d**) Neo and BI-1 cells were cultured in serum-free medium with 5 ng/ml TGF-β1 for 0, 12, 24, 36, or 48 h. After isolating a pure ER fraction, α-glucosidase, ER-resident mannosidase or UDP glucuronsyltransferase activity was analyzed as described in the Materials and Methods. *$P<0.05$, significantly different from Neo cells at each time point. (**e**) Neo and BI-1 cells were cultured in serum-free medium with 5 ng/ml TGF-β1 for 0, 12, 24, 36, or 48 h, and immunoblotting was performed with anti-calreticulin or calnexin antibodies. β-Actin antibody staining of the same loading was used as a control. (**f**) Neo and BI-1 cells were cultured in serum-free medium with 5 ng/ml TGF-β1 for 0, 24, or 48 h. Lysates were subjected to immunoprecipitation and immunoblotting with anti-V-ATPase or calnexin antibody

highly expressed in airway epithelial cells, alveolar macrophages, and fibroblasts of BI-1$^{-/-}$ mice than those of BI-1$^{+/+}$ mice (Supplementary Figure S6a). CHOP, another ER stress protein, was more highly expressed in bleomycin-treated BI-1$^{-/-}$ mice than in bleomycin-treated BI-1$^{+/+}$ mice. In immunoblot analysis, GRP78, CHOP, p-eIF-2α, IRE-1α, and spliced XBP-1 were more highly expressed in the lung tissues of bleomycin-treated BI-1$^{-/-}$ mice than in bleomycin-treated BI-1$^{+/+}$ mice (Supplementary Figure S6b). The pro-form of ATF-6α, p90, was expressed at lower levels in BI-1$^{-/-}$ mice than in BI-1$^{+/+}$ mice. Total number of alveolar inflammatory cells was higher in bronchoalveolar lavage fluid samples from BI-1$^{-/-}$ mice than those from BI-1$^{+/+}$ mice treated with bleomycin (Supplementary Table S1); there was

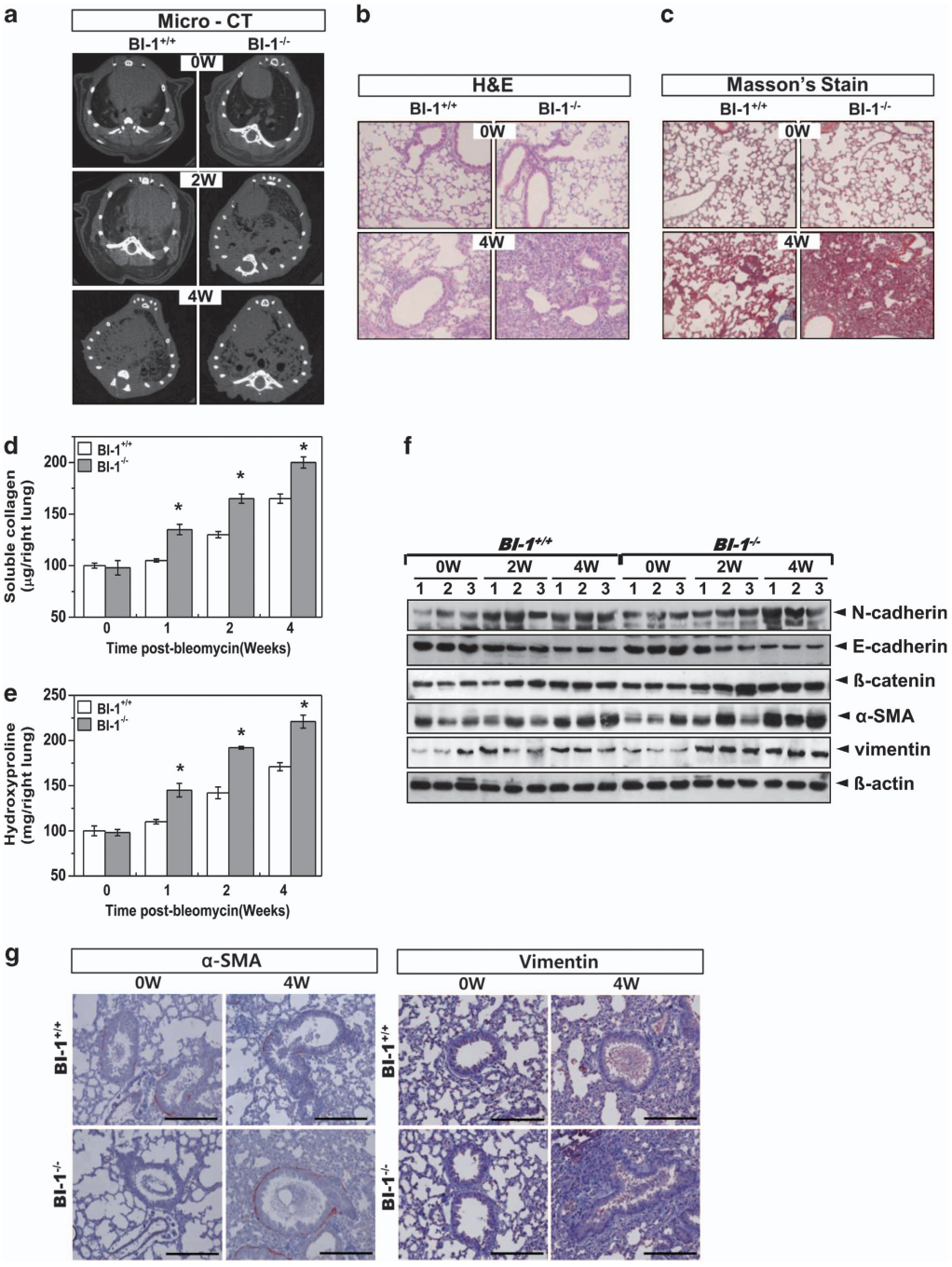

Figure 7 BI-1 regulates bleomycin-induced pulmonary fibrosis. BI-1$^{+/+}$ and BI-1$^{-/-}$ mice were treated by intratracheal injection of bleomycin (0.5 U/kg) for the indicated number of weeks. Control group were injected with the same volume of sterile saline. (**a**) Micro-CT analysis was performed, and representative micro-CT images from bleomycin-treated or non-treated BI-1$^{+/+}$ and BI-1$^{-/-}$ lungs are shown. Lung sections were stained (**b**) with hematoxylin and eosin and, for collagen deposition, (**c**) with Masson's trichrome ($\times$ 200 magnification). (**d**) Total soluble collagen and (**e**) hydroxyproline were measured as described in the Materials and Methods. *$P<0.05$, significantly different from BI-1$^{+/+}$ lungs at each time point. (**f**) Immunoblotting of lung lysates was performed after 0, 2, or 4 weeks of bleomycin treatment of BI-1$^{+/+}$ and BI-1$^{-/-}$ mice using anti-E-cadherin, N-cadherin, β-catenin, α-SMA, or vimentin antibodies. β-Actin antibody staining of the same loading was used as a control. (**g**) Lung sections were immunostained with anti-SMA or vimentin antibody

a greater increase in the number of macrophages and lymphocytes in the fluid samples from BI-1$^{-/-}$ mice than those from BI-1$^{+/+}$ mice. Concentration of TGF-β in bronchoalveolar lavage fluid was significantly higher in bleomycin-treated mice than in non-treated mice and was higher in BI-1$^{-/-}$ mice than in BI-1$^{+/+}$ mice.

BI-1 regulates pulmonary fibrosis through enhanced ER folding capacitance-associated lysosomal V-ATPase glycosylation. Expression of proteasome 20S did not differ between BI-1$^{+/+}$ and BI-1$^{-/-}$ mice (Supplementary Figure S7). Lysosomal morphology was examined via electron microscopic analysis. In the bleomycin-treated groups,

lysosome size and number were decreased, but these alterations were more severe in BI-1$^{-/-}$ mice than in BI-1$^{+/+}$ mice (Figure 8a). Lysosomes were partially broken in mice treated with bleomycin for 4 weeks, especially in BI-1$^{-/-}$ mice. Lysosomal enzyme activity was also examined *in vivo*. Cathepsin B and K activities were highly induced in the lungs of bleomycin-treated BI-1$^{+/+}$ mice compared with the lungs of bleomycin-treated BI-1$^{-/-}$ mice (Figure 8b). V-ATPase activity, which contributes to the maintenance of an acidic vesicle environment, was highly induced in bleomycin-treated BI-1$^{+/+}$ mice but was decreased in BI-1$^{-/-}$ mice (Figure 8c). The activities of β-galactosidase and α-mannosidase, which are glycosylation-associated enzymes, were significantly induced in BI-1$^{+/+}$ mice as compared with that in BI-1$^{-/-}$ mice (Figure 8d).

Immunoblotting indicated that expression of glycosylated V-ATPase was maintained at a relatively high level in bleomycin-treated BI-1$^{+/+}$ mice. Immature V-ATPase expression was higher in BI-1$^{-/-}$ mice than in BI-1$^{+/+}$ mice (Figure 8e). In addition, calnexin, a key cofactor for mannosidase, was expressed at higher levels in BI-1$^{+/+}$ mice than in BI-1$^{-/-}$ mice, but the expression of calreticulin, another chaperone protein, was not significantly altered by bleomycin treatment. Next, we examined the interaction between V-ATPase and calnexin in the knockout mice. In BI-1$^{-/-}$ mice, the basal interaction between V-ATPase and calnexin was similar to that in BI-1$^{+/+}$ mice. During the 2-week treatment period, binding between V-ATPase and calnexin increased similarly in BI-1$^{+/+}$ and BI-1$^{-/-}$ mice (Figure 8f). However, the interaction in BI-1$^{-/-}$ mice increased significantly compared with that in BI-1$^{+/+}$ mice, especially at 4 weeks, suggesting that folding requirements due to the accumulation of immature proteins may increase during pulmonary fibrosis processes, leading to a more severe ER stress response in BI-1$^{-/-}$ mice than in BI-1$^{+/+}$ mice (Supplementary Figures S6a and b). Consistent with the *in vitro* results, these *in vivo* data suggest that BI-1 stimulates V-ATPase glycosylation, thereby enhancing V-ATPase activity and collagen degradation.

Discussion

In this study, we demonstrated in both *in vitro* and *in vivo* fibrosis models that BI-1 functions as a glycosylation enhancer and ER stress regulator, thereby affecting collagen catabolism and the EMT.

In the presence of BI-1, we observed less accumulation of collagen along with enhanced protein degradation activity. A common feature of IPF is an imbalance in the normal homeostasis of the ECM, mainly collagen, so that synthesis exceeds breakdown, resulting in excessive accumulation of collagen.[25] It has been suggested that in IPF patients the persistence and progression of fibrosis is probably due to a decrease in collagen degradation.[26] The accumulation of collagen has already been established as a pathological mechanism for IPF. In our TGF-β-induced EMT model, BI-1-enhanced collagen degradation was linked to lysosomal V-ATPase maturation (Figures 1 and 2). We hypothesized that V-ATPase, a core protein involved in the acidification of intracellular organelles, has a regulatory role in the post-translational degradation of collagen. V-ATPase is an *N*-acetylglycosylated protein. During maturation, the V-ATPase is translocated into cellular organelles, such as lysosomes. In BI-1 cells, V-ATPase appeared to be more successfully translocated into lysosomes than in Neo cells, as indicated by our subcellular fraction and confocal analysis results (Figures 5b and c). In response to TGF-β1 treatment, which induces an ER stress state, an unglycosylated portion of V-ATPase was also detected in lysosome fractions, especially those from Neo cells. Although unglycosylated proteins ideally should not be translocated to their final destination, some misfolded proteins, including unglycosylated V-ATPase, seem to be able to translocalize to their destination organelles.[27] V-ATPase glycosylation and the rate-limiting enzymes for glycosylation, including glucosidase and ER-resident mannosidase, were more highly activated in BI-1 cells than in Neo cells (Figure 6d). Mannosidase activation is an essential part of normal glycoprotein maturation in the ER and is the final glycan processing step before it is transported to the Golgi. Calnexin, a chaperone protein required for mannosidase activity, which itself is the rate-limiting step for *N*-acetylglycosylation, was also highly expressed in BI-1 cells, and its expression was more stable in the presence of TGF-β1 in BI-1 cells than in Neo cells. Although calnexin expression was higher in BI-1 cells, V-ATPase was more easily dissociated from calnexin in BI-1 cells than in Neo cells, indicating that the mature/glycosylated form of V-ATPase was not stably associated with the ER-localized chaperone protein (Figure 6f). Folding of several other *N*-glycosylated proteins via interactions with calnexin and calreticulin has been studied under various conditions.[28,29] In this study, we suggest that a BI-1-associated glycosylation environment has a role in maturation of the V-ATPase, resulting in enhanced collagen degradation and regulation of the EMT.

BI-1 has been proposed to be a Ca^{2+} channel-like protein/Ca^{2+}/H^+ antiporter.[30,31] It has been suggested that increased $[H^+]_{ER}$ uptake, facilitated by BI-1, enhances intra-ER folding capacity, leading to protein maturation and more efficient translocation of V-ATPase into lysosomes.[32] Maintenance of Ca^{2+} homeostasis in the ER is essential for protein folding. One of the main characteristics of BI-1 is that it stabilizes intra-ER Ca^{2+} homeostasis through Ca^{2+} leakage and counter-activation of Ca^{2+}-ATPases (unpublished data). Dimerization of BI-1 seems to enhance Ca^{2+} channel characteristics.[19,33] In this study, BI-1 dimerized in BI-1-overexpressing cells (data not shown). Dynamic movement of Ca^{2+} in BI-1 cells may be related to elevated expression of the lectin family protein, calnexin. Lectin proteins, including calreticulin and calnexin, modulate Ca^{2+} oscillations, suggesting communication between the Ca^{2+} signaling system and the folding machinery in the ER.[34–36] Our results suggest that calnexin enhances the lysosomal protease environment, leading to collagen degradation in the context of BI-1-enhanced V-ATPase glycosylation.

Throughout this study, we discussed V-ATPase glycosylation and its associated lectin protein, calnexin, with respect to the BI-1-enhanced lysosome-related degradation pathway. To confirm the *in vitro* phenomena and their suggested mechanisms, we performed *in vivo* investigations.

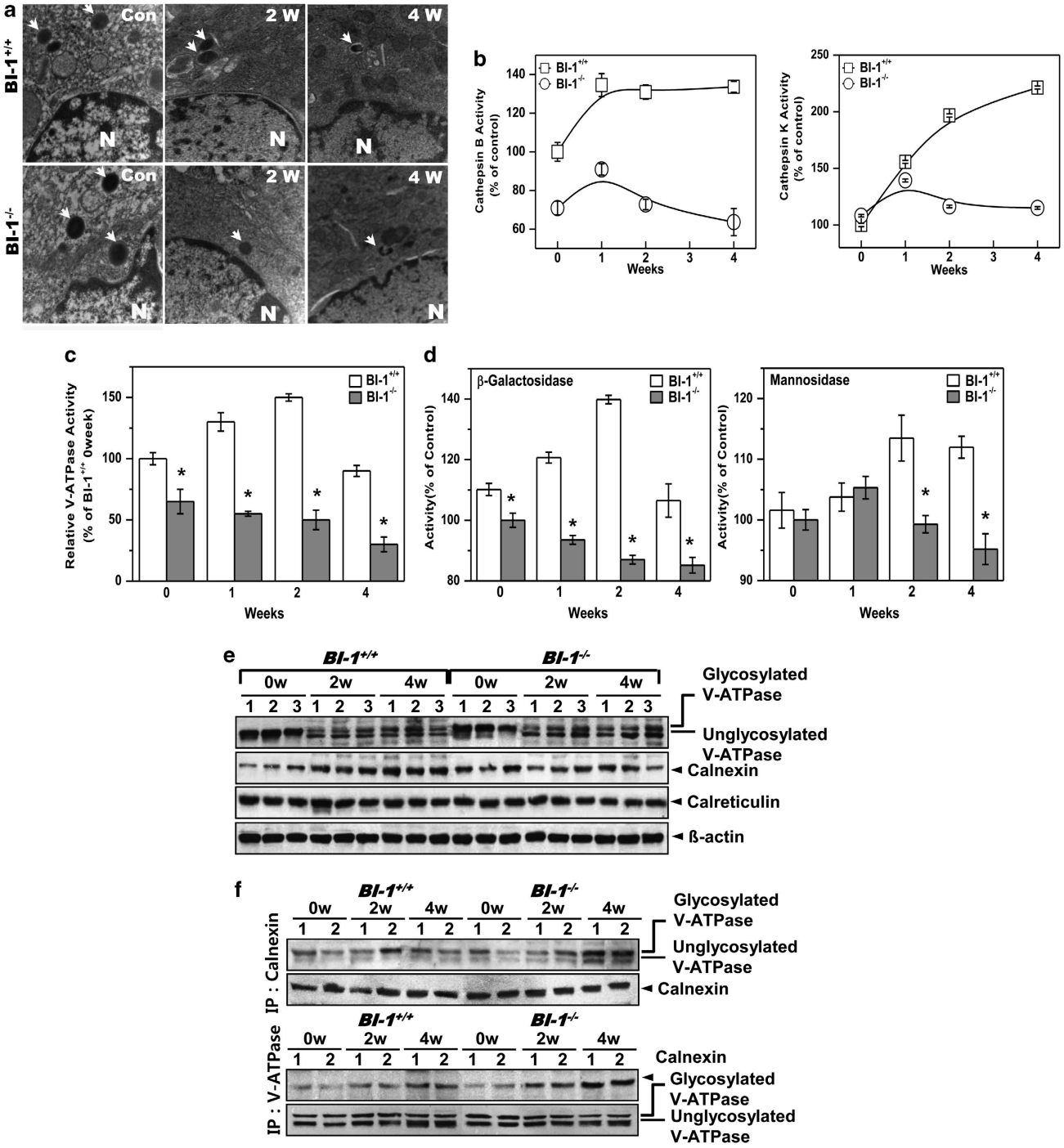

Figure 8 BI-1 regulates lung fibrosis through enhanced ER folding capacitance-associated lysosomal V-ATPase glycosylation. BI-1 $^{+/+}$ and BI-1 $^{-/-}$ mice were treated by intratracheal injection of bleomycin (0.5 U/kg) for the indicated number of weeks. (**a**) Electron microscopy was performed as described in the Materials and Methods. (**b**) After isolation of lysosomes from lung tissue, cathepsin B and K enzyme activities were analyzed. (**c**) To assess lysosomal V-ATPase activity, 6 μM acridine orange solution was added to lysosomal membranes from the lung tissues of bleomycin-treated or non-treated mice for the indicated periods. Intra-vesicular H^+ uptake was initiated by the addition of Mg-ATP. Lysosomal V-ATPase activity was analyzed as described in the Materials and Methods. *$P<0.05$, significantly different from ATP-exposed BI-1 $^{+/+}$ control mice. (**d**) β-Galactosidase and α-mannosidase activities were measured in pure lysosomal extracts. *$P<0.05$, significantly different from ATP-exposed BI-1 $^{+/+}$ control mice. (**e**) Immunoblotting of lung lysates from BI-1 $^{+/+}$ and BI-1 $^{-/-}$ mice treated with bleomycin for 0, 2, or 4 weeks was performed using antibodies against V-ATPase, calnexin, and calreticulin. (**f**) Immunoprecipitation and immunoblotting of the lysates were performed using anti-V-ATPase or calnexin antibody

Collagen accumulated to a significantly greater extent in BI-1 $^{-/-}$ mice than in BI-1 $^{+/+}$ mice (Figure 7d). We also demonstrated that BI-1 is involved in the maintenance of lysosome characteristics, including lysosomal structures and the activities of enzymes, such as cathepsins, V-ATPase, and glycosylation-related enzymes (Figures 8a–d). Regulation of

glycosylated V-ATPase, calnexin expression, and their interaction were confirmed in BI-1$^{-/-}$ mice, and the results were consistent with our *in vitro* findings. However, endogenous expression of BI-1 and its role still need to be studied in IPF patients to validate our findings.

In summary, BI-1 regulated the TGF-β1-induced EMT phenomenon in an *in vitro* model of IPF as well as an *in vivo* model of bleomycin-induced lung fibrosis. BI-1 regulated EMT by regulating the Ca^{2+} dynamic status and the expression of calnexin, which is linked to mannosidase activation and resultant glycosylation in pulmonary systems. Further studies of BI-1 will contribute to our understanding of the mechanism of IPF and potentially lead to the development of BI-1 enhancers or agonists for the treatment of IPF.

Materials and Methods

Materials. Recombinant human TGF-β1 and anti-goat cadherin antibody were purchased from R&D Systems (Minneapolis, MN, USA). A mouse monoclonal antibody against human N-cadherin was purchased from BD Transduction Laboratory (Oxford, UK). Anti-rabbit β-catenin antibody was obtained from ABcam Ltd. (Cambridge, UK). Anti-rabbit polyclonal antibody against mouse N-cadherin was provided by ABcam Ltd. Anti-rabbit polyclonal β-catenin, calreticulin, and collagen antibodies for immunostaining were also obtained from ABcam Ltd. Anti-rabbit E-cadherin and vimentin antibodies were purchased from Cell Signaling Inc. (Danvers, MA, USA). Anti-rabbit polyclonal V-ATPase antibody for immunoblotting was purchased from Synaptic Systems (Goettingen, Germany). Anti-mouse collagen antibody for immunoblotting, anti-mouse monoclonal V-ATPase antibody for immunostaining, β-actin antibody, anti-rabbit polyclonal calnexin antibody, anti-rat monoclonal LAMP-1 antibody, anti-rat monoclonal GRP78 antibody, anti-rabbit polyclonal CHOP antibody, and anti-mouse monoclonal SMA antibody were supplied by Santa Cruz Biotechnology (Santa Cruz, CA, USA). Bleomycin was purchased from Sigma-Aldrich (St. Louis, MO, USA). All other chemicals were purchased from Sigma (St. Louis, MO, USA). The purities of all reagents were at least of analytical grade.

Cell culture and transfection. Human type II alveolar epithelial cells (A549) were purchased from and maintained as instructed by the Korean Cell Line Bank (Seoul, Korea). Human A549 cells were stably transfected with pcDNA3 or pcDNA3-BI-1 plasmids using Superfect transfection reagent (QIAamp Viral RNA Mini Kit, Qiagen, Venlo, Netherlands). Cells were then cultured for 3 weeks in 1 mg/ml G418 (Invitrogen, Carlsbad, CA, USA). Cells were maintained in Dulbecco's modified Eagle's medium (DMEM) (Gibco BRL, Gaithersburg, MD, USA) supplemented with penicillin and streptomycin (100 U/ml) with 10% fetal bovine serum (Gibco) and grown at 37 °C in a humidified, 5% CO_2 atmosphere. siRNA reagents targeting V-ATPase (or non-specific siRNA) were purchased from Santa Cruz Biotechnology and delivered into A549 cells at a final concentration of 100 nM using the Amaxa nucleofection device (Buffer R, Program A-24, Lonza, Wokingham, UK) according to the manufacturer's instructions. Knockdown efficiency was then assessed by western blotting 24 h after transfection.

Fluorescence microscopic analysis. Cells were washed three times in phosphate-buffered saline (PBS), fixed in 95% ethanol, permeabilized in 0.1% (vol/vol) Triton X-100, blocked in 3% bovine serum albumin, and then incubated with rhodamine-conjugated phalloidin (Invitrogen). Separately, cells were incubated with E-cadherin, N-cadherin, or SMA antibody (primary antibody, 1 : 1000 in blocking buffer) for 2 h at room temperature. Cells were then washed three times in PBS and incubated for 1 h at room temperature with appropriate IgG secondary antibodies (1 : 200). Fluorescent images were obtained with an Olympus FluoView 300 laser-scanning confocal microscope (Olympus, New York, NY, USA).

Western blotting. Western blotting analyses were performed as described previously.[33] All western blotting procedures are described in detail in the Supplementary Information.

Collagen assay. We used the colorimetric Sircol soluble collagen assay (Biocolor Ltd., Carrickfergus, UK), which is based on dye that binds specifically to the native triple helix structure of collagen, to quantify collagen levels. We added the dye in excess amounts to supernatant cell culture medium or cell membrane preparations and mixed thoroughly. We centrifuged the dye/sample mix (10 000 $\times$ *g* for 10 min) to obtain a pellet of collagen with bound dye and discarded the supernatant with unbound dye. We dissolved the pellet in an acidic solution provided with the kit and measured the photometric absorbance of the dyed solution, which is directly proportional to the amount of collagen present in the sample.

Hydroxyproline assay. The amount of hydroxyproline, which is directly proportional to the collagen content, was measured as described previously.[37]

Degradation of collagen by lysosomal membrane fractions. Type I collagen (0.5 mg/ml) was purified from rat tails as described previously.[21,38] Type I collagen (0.4 mg/ml) was incubated with the lysosomal membrane fraction (500 μg) from Neo or BI-1 cells in 100 mM sodium acetate, pH 5.5 buffer containing 2.5 mM DTT and 2.5 mM EDTA at 37 °C. Degrees of digestion at a given incubation time were analyzed. Reaction was stopped by the addition of 2.0 M Tris-HCl buffer (pH 9.0) to give a final concentration of 0.2 M. Then, samples were subjected to sodium dodecyl sulfate (SDS)-PAGE.

PNGase-F digestion. Samples were placed in buffer containing NP-40, 0.3% SDS, 0.6% β-mercaptoethanol, and digested overnight at 37 °C with or without 100 units of PNGase F (New England Biolabs, Ipswich, MA, USA) per μg of protein. Controls were treated identically to experimental samples but without addition of PNGase-F. Proteins were diluted directly into Laemmli sample buffer for analysis by SDS-PAGE.

Gel staining. Degree of digestion was monitored by staining SDS-PAGE gels with silver nitrite[39] and Coomassie Brilliant Blue. Gels were stained for 5 min in 1 mg/ml Coomassie Brilliant Blue or for 30 min in 2 mg/ml silver nitrite in 50% methanol and destained in 50% methanol until bands were visible.

RNA isolation and real-time PCR analysis. All detailed RNA isolation and real-time PCR procedures are described in the Supplementary Information.

Methionine-labeled protein synthesis analysis. Cells were labeled with [^{35}S] methionine (1000 Ci/mmol, 500 μCi/ml) for 1.5 h in methionine-free DMEM supplemented with 10% FBS. After labeling, cells were washed with DMEM, trypsinized, and then run on SDS gradient gels.

Assessing lysosome activity by microscopy. LysoTracker probes are fluorescent acidotropic probes for labeling and tracking acidic organelles in live cells. These probes have high selectivity for acidic organelles and can effectively label live cells. Cells were grown in cell culture dishes, rinsed with PBS, and stained with 100 nM LysoTracker Green DND-26 (Molecular Probes, Eugene, OR, USA) in serum-free medium for 30 min at room temperature. Cells were then washed with PBS, and lysosomal intensity was analyzed by fluorescence microscopy (Olympus) at 488 nm. Images of red fluorescent cells were acquired using a digital charge-coupled device color video camera (CCS-212, Samsung, Seoul, Korea), captured, and then transferred to a computer using the WinFast 3D S680 frame grabber (Leadtek, Taipei, Taiwan). Fluorescence values of 100 randomly selected cell images were measured for each condition. Intensity of lysosome fluorescence in the cells was expressed as the ratio of the average fluorescence of 100 treated cells to the fluorescence of 100 control cells.

Lysosomal V-ATPase activity assessment. We measured lysosomal V-ATPase activity using previously described procedures with some modifications.[40,41] Isolated lysosomes from TGF-β1-treated or non-treated Neo or BI-1 cells or from bleomycin-treated or non-treated BI-1$^{+/+}$ and BI-1$^{-/-}$ mice lung tissues were placed in a cuvette containing activation buffer and 6.7 μM acridine orange. After achieving a steady spectrofluorometric baseline, V-ATPase was activated by the addition of ATP (to a final concentration of 1.4 μM) and valinomycin. Valinomycin treatment causes membrane potential generation by promoting the efflux of K^+ from cells. For V-ATPase activity, the V-ATPase-driven pumping of hydrogen ions into lysosomes was measured by acridine orange fluorescence quenching (excitation at 495 nm; emission at 530 nm) using an integrated spectrofluorometer (Photon Technology International, Birmingham, NJ, USA).

Lysosomal cathepsin assays. Inhibitory activity against cathepsins B and K was assayed fluorometrically using the Molecular Devices Gemini XS system, with an excitation wavelength of 350 nm and an emission wavelength of 460 nm, as described previously.[42]

Lysosomal β-galactosidase, α-mannosidase, and β-glucuronidase assays. Lysosomal proteins were suspended in 200 μl of 100 mM phosphate–citrate buffer (pH 4.3) for β-galactosidase and α-mannosidase assays and in 200 μl of 100 mM acetate buffer (pH 4.5) for β-glucuronidase assays. Cells were sonicated three times with an ultrasonic cell disrupter for 20 s on ice, and then cell lysates were centrifuged at 12 000 $\times$ *g* for 10 min at 4 °C. The following substrates were used to determine enzyme activity: *p*-nitrophenyl-b-D-glucuronide (Fluka Chemie; Sigma) for β-glucuronidase, *p*-nitrophenyl-b-D-galactopyranoside (Sigma) for β-galactosidase, and *p*-nitrophenyl-a-D-mannopyranoside for α-mannosidase (Sigma).

ER-resident enzyme analysis. α-Glucosidase activity of ER fractions was analyzed as described by Rolfsmeier and Blum (1995) using *p*-nitrophenyl-α-D-glucopyranoside as a substrate,[43] and ER-resident mannosidase activity was measured using *p*-nitrophenyl-α-D-mannopyranoside and M9GlcNAc2-Asn oligosaccharides as described previously.[44]

Induction of the animal model. Six male BI-1$^{+/+}$ and six male BI-1$^{-/-}$ mice were used for the micro-CT scans. Another five male BI-1$^{+/+}$ and five male BI-1$^{-/-}$ mice were used for immunohistochemistry. In preparation for treatment with bleomycin solution (0.5 U/kg), mice (four treated and two control) were anesthetized with ketamine (56 mg/kg, IP) and rompun (2.8 mg/kg, IP) and intubated. A catheter was placed through the intubation tube pointing toward the left lung. A solution of bleomycin and saline was instilled into the left lung, and the animal was placed on its left side for 2 min. Control animals were treated with saline only. Animals were monitored continuously for signs of distressed breathing and kept warm under a heat lamp until fully recovered. All procedures were approved by the Institutional Animal Care and Use Committee of Chonbuk National University.

Histological examination. All detailed histological examination procedures are described in the Supplementary Information.

Bronchoalveolar lavage fluid cell count. Two weeks after bleomycin instillation, mice were euthanized by injection of a lethal dose of pentobarbital. Lungs were flushed three times with 0.6 ml of ice-cold Dulbecco's PBS, the recovered fluid was centrifuged, and the cell pellet was re-suspended in 1 ml of ice-cold saline. A total cell count was performed using a Neubauer counting chamber (depth = 0.1 mm, area = 0.0025 mm^2; Optik Labor, Friedrichshofen, Germany). For differential cell count cells, a constant volume of 0.2 ml PBS was transferred to a glass slide with a Cytospin-3 centrifuge (Shandon Scientific Ltd., Runcorn, UK) and stained with May Gruenwald/Giemsa. Numbers of macrophages, neutrophils, and lymphocytes were counted from among 100 total cells using a light microscope (Leica, Wetzlar, Germany). These data were then extrapolated to determine the number of cells per milliliter.

Statistical analyses. Statistical differences in acidity level-response experiments were evaluated by analysis of variance and two-tailed Student's *t*-tests.

Conflict of Interest

The authors declare no conflict of interest.

Acknowledgements. This study was supported by grants (2012R1A2 A1A03001907) from the National Research Foundation of Korea and, in part, by a grant from Korea Healthcare Technology, Ministry for Health, Welfare and Family Affairs (A121931).

Author contributions

The project was formulated by HJC. HJC and HRK wrote the manuscript. MRL, GHL, HYL, and DSK performed the experiments. MJC and YCL discussed the study design and provided materials for this study. All authors read the final manuscript and agreed with the decision to submit.

1. Kropski JA, Lawson WE, Young LR, Blackwell TS. Genetic studies provide clues on the pathogenesis of idiopathic pulmonary fibrosis. *Dis Models Mech* 2013; **6**: 9–17.
2. Krein PM, Winston BW. Roles for insulin-like growth factor I and transforming growth factor-beta in fibrotic lung disease. *Chest* 2002; **122**(6 Suppl): 289S–293S.
3. Yang K, Palm J, Konig J, Seeland U, Rosenkranz S, Feiden W *et al.* Matrix-metallo-proteinases and their tissue inhibitors in radiation-induced lung injury. *Int J Radiat Biol* 2007; **83**: 665–676.
4. Kage H, Borok Z. EMT and interstitial lung disease: a mysterious relationship. *Curr Opin Pulm Med* 2012; **18**: 517–523.
5. Decologne N, Wettstein G, Bonniaud P. [A role for mesothelial cells in the genesis of idiopathic pulmonary fibrosis?]. *Bull Acad Natl Med* 2010; **194**: 383–389.
6. Lekkerkerker AN, Aarbiou J, van Es T, Janssen RA. Cellular players in lung fibrosis. *Curr Pharm Des* 2012; **18**: 4093–4102.
7. Cheresh P, Kim SJ, Tulasiram S, Kamp DW. Oxidative stress and pulmonary fibrosis. *Biochim Biophys Acta* 2013; **1832**: 1028–1040.
8. Cui Y, Robertson J, Maharaj S, Waldhauser L, Niu J, Wang J *et al.* Oxidative stress contributes to the induction and persistence of TGF-beta1 induced pulmonary fibrosis. *Int J Biochem Cell Biol* 2011; **43**: 1122–1133.
9. Lawson WE, Cheng DS, Degryse AL, Tanjore H, Polosukhin VV, Xu XC *et al.* Endoplasmic reticulum stress enhances fibrotic remodeling in the lungs. *Proc Natl Acad Sci USA* 2011; **108**(26): 10562–10567.
10. Tanjore H, Lawson WE, Blackwell TS. Endoplasmic reticulum stress as a pro-fibrotic stimulus. *Biochim Biophys Acta* 2013; **1832**: 940–947.
11. Tanjore H, Blackwell TS, Lawson WE. Emerging evidence for endoplasmic reticulum stress in the pathogenesis of idiopathic pulmonary fibrosis. *Am J Physiol Lung Cell Mol Physiol* 2012; **302**: L721–L729.
12. Reimers K, Choi CY, Bucan V, Vogt PM. The Bax inhibitor-1 (BI-1) family in apoptosis and tumorigenesis. *Curr Mol Med* 2008; **8**: 148–156.
13. Kim HR, Lee GH, Ha KC, Ahn T, Moon JY, Lee BJ *et al.* Bax inhibitor-1 is a pH-dependent regulator of Ca2+ channel activity in the endoplasmic reticulum. *J Biol Chem* 2008; **283**: 15946–15955.
14. Bultynck G, Kiviluoto S, Henke N, Ivanova H, Schneider L, Rybalchenko V *et al.* The C terminus of Bax inhibitor-1 forms a Ca2+-permeable channel pore. *J Biol Chem* 2012; **287**: 2544–2557.
15. Michalak M, Groenendyk J, Szabo E, Gold LI, Opas M. Calreticulin, a multi-process calcium-buffering chaperone of the endoplasmic reticulum. *Biochem J* 2009; **417**: 651–666.
16. Nomura R, Orii M, Senda T. Calreticulin-2 is localized in the lumen of the endoplasmic reticulum but is not a Ca2+ -binding protein. *Histochem Cell Biol* 2011; **135**: 531–538.
17. Malhotra JD, Kaufman RJ. The endoplasmic reticulum and the unfolded protein response. *Semin Cell Dev Biol* 2007; **18**: 716–731.
18. Lawson WE, Crossno PF, Polosukhin VV, Roldan J, Cheng DS, Lane KB *et al.* Endoplasmic reticulum stress in alveolar epithelial cells is prominent in IPF: association with altered surfactant protein processing and herpesvirus infection. *Am J Physiol Lung Cell Mol Physiol* 2008; **294**: L1119–L1126.
19. Baek HA, Kim do S, Park HS, Jang KY, Kang MJ, Lee DG *et al.* Involvement of endoplasmic reticulum stress in myofibroblastic differentiation of lung fibroblasts. *Am J Respir Cell Mol Biol* 2012; **46**: 731–739.
20. Balestrini JL, Chaudhry S, Sarrazy V, Koehler A, Hinz B. The mechanical memory of lung myofibroblasts. *Integr Biol (Camb)* 2012; **4**: 410–421.
21. Hwang HS, Chung HS. Preparation of active recombinant cathepsin K expressed in bacteria as inclusion body. *Protein Expr Purif* 2002; **25**: 541–546.
22. Lee GH, Kim HR, Chae HJ. Bax inhibitor-1 regulates the expression of P450 2E1 through enhanced lysosome activity. *Int J Biochem Cell Biol* 2012; **44**: 600–611.
23. Efeyan A, Zoncu R, Sabatini DM. Amino acids and mTORC1: from lysosomes to disease. *Trends Mol Med* 2012; **18**: 524–533.
24. Trombetta ES, Helenius A. Lectins as chaperones in glycoprotein folding. *Curr Opin Struct Biol* 1998; **8**: 587–592.
25. Selman M, Montano M, Ramos C, Chapela R. Concentration, biosynthesis and degradation of collagen in idiopathic pulmonary fibrosis. *Thorax* 1986; **41**: 355–359.
26. Montano M, Ramos C, Gonzalez G, Vadillo F, Pardo A, Selman M. Lung collagenase inhibitors and spontaneous and latent collagenase activity in idiopathic pulmonary fibrosis and hypersensitivity pneumonitis. *Chest* 1989; **96**: 1115–1119.
27. Cui F, Liu L, Zhao Q, Zhang Z, Li Q, Lin B *et al.* Arabidopsis ubiquitin conjugase UBC32 is an ERAD component that functions in brassinosteroid-mediated salt stress tolerance. *Plant Cell* 2012; **24**: 233–244.
28. Zhang Q, Salter RD. Distinct patterns of folding and interactions with calnexin and calreticulin in human class I MHC proteins with altered N-glycosylation. *J Immunol* 1998; **160**: 831–837.
29. Joseph SK, Boehning D, Bokkala S, Watkins R, Widjaja J. Biosynthesis of inositol trisphosphate receptors: selective association with the molecular chaperone calnexin. *Biochem J* 1999; **342**(Pt 1): 153–161.
30. Ahn T, Yun CH, Kim HR, Chae HJ. Cardiolipin, phosphatidylserine, and BH4 domain of Bcl-2 family regulate Ca2+/H+ antiporter activity of human Bax inhibitor-1. *Cell Calcium* 2010; **47**: 387–396.

31. Lee GH, Ahn T, Kim DS, Park SJ, Lee YC, Yoo WH *et al.* Bax inhibitor 1 increases cell adhesion through actin polymerization: involvement of calcium and actin binding. *Mol Cell Biol* 2010; **30**: 1800–1813.
32. Lee GH, Kim DS, Kim HT, Lee JW, Chung CH, Ahn T *et al.* Enhanced lysosomal activity is involved in Bax inhibitor-1-induced regulation of the endoplasmic reticulum (ER) stress response and cell death against ER stress: involvement of vacuolar H + -ATPase (V-ATPase). *J Biol Chem* 2011; **286**: 24743–24753.
33. Kim HR, Lee GH, Cho EY, Chae SW, Ahn T, Chae HJ. Bax inhibitor 1 regulates ER-stress-induced ROS accumulation through the regulation of cytochrome P450 2E1. *J Cell Sci* 2009; **122**(Pt 8): 1126–1133.
34. Roderick HL, Lechleiter JD, Camacho P. Cytosolic phosphorylation of calnexin controls intracellular Ca(2 +) oscillations via an interaction with SERCA2b. *J Cell Biol* 2000; **149**: 1235–1248.
35. Camacho P, Lechleiter JD. Calreticulin inhibits repetitive intracellular Ca2 + waves. *Cell* 1995; **82**: 765–771.
36. John LM, Lechleiter JD, Camacho P. Differential modulation of SERCA2 isoforms by calreticulin. *J Cell Biol* 1998; **142**: 963–973.
37. Umino T, Wang H, Zhu Y, Liu X, Manouilova LS, Spurzem JR *et al.* Modification of type I collagenous gels by alveolar epithelial cells. *Am J Respir Cell Mol Biol* 2000; **22**: 702–707.
38. Rajan N, Habermehl J, Cote MF, Doillon CJ, Mantovani D. Preparation of ready-to-use, storable and reconstituted type I collagen from rat tail tendon for tissue engineering applications. *Nat Protoc* 2006; **1**: 2753–2758.
39. Thiede B, Kretschmer A, Rudel T. Quantitative proteome analysis of CD95 (Fas/Apo-1)-induced apoptosis by stable isotope labeling with amino acids in cell culture, 2-DE and MALDI-MS. *Proteomics* 2006; **6**: 614–622.
40. Cox BE, Griffin EE, Ullery JC, Jerome WG. Effects of cellular cholesterol loading on macrophage foam cell lysosome acidification. *J Lipid Res* 2007; **48**: 1012–1021.
41. Crider BP, Xie XS. Characterization of the functional coupling of bovine brain vacuolar-type H(+)-translocating ATPase. Effect of divalent cations, phospholipids, and subunit H (SFD). *J Biol Chem* 2003; **278**: 44281–44288.
42. Kulig P, Kantyka T, Zabel BA, Banas M, Chyra A, Stefanska A *et al.* Regulation of chemerin chemoattractant and antibacterial activity by human cysteine cathepsins. *J Immunol* 2011; **187**: 1403–1410.
43. Rolfsmeier M, Blum P. Purification and characterization of a maltase from the extremely thermophilic crenarchaeote *Sulfolobus solfataricus*. *J Bacteriol* 1995; **177**: 482–485.
44. Mora-Montes HM, Lopez-Romero E, Zinker S, Ponce-Noyola P, Flores-Carreon A. Hydrolysis of Man9GlcNAc2 and Man8GlcNAc2 oligosaccharides by a purified alpha-mannosidase from *Candida albicans*. *Glycobiology* 2004; **14**: 593–598.

Supplementary Information accompanies this paper on Cell Death and Disease website (http://www.nature.com/cddis)